



# Energy harvester based on low cost piezoelectric membrane for road traffic application

Ernest Bernat-Maso<sup>1</sup> · Borja Martínez<sup>1</sup> · Luis Mercedes<sup>1</sup> · Virginia Mendizábal<sup>1</sup>

Received: 6 September 2022 / Accepted: 7 June 2023 / Published online: 24 June 2023  
© The Author(s) 2023

## Abstract

Piezoelectric harvesters are environmentally sustainable alternative electrical production technologies aimed at supplying small autonomous devices. The particular application in roads has significant potential. However, there are discrepancies about the effectiveness of these harvesters, and their costs limit their market expansion abilities. In this context, a novel harvester approach is explored that includes low-cost membrane piezoelectric patches in modified cymbal devices. The main novelty of this approach is the inclusion of an inner contact column that punctually transmits the load of the caps of the cymbal to the centre of the membrane piezoelectric patch, maximising its deformation and energy production capabilities. Experimental tests on piezoelectric elements, harvesters and embedder harvesting units have been performed with numerical simulations to optimise the design of the harvester. The results indicate that the more punctual the inner contact column is, the more electrical energy is produced, reaching values ten times greater than those of the present cymbal configuration. Embedding the harvester into a flexible pavement and positioning it under a wheel track are beneficial aspects of the execution. Finally, the dependency on the wheel speed is confirmed with wheel-track tests on a representative pad of the system.

## 1 Introduction

Developing efficient sustainable energy production technologies is one of the main social challenges to date. Although there are some commercial solutions using solar, sea or wind energies, there is still a wide range of possibilities to be developed or scaled to practical applications. This case is true for piezoelectric-based energy harvesting alternatives. This concept includes a wide range of systems based on turning input mechanical energy into electrical energy by using the piezoelectric effect.

In this context, piezoelectric road energy harvesting is interesting because of several advantages. First, this system can be installed on remote points of road networks that are not reached by the electric distribution infrastructure. Thus, this technique allows the creation of an electrical supply point where it is not currently available for use in activities related to traffic use. In addition, the production of

electricity is based on harvesting the mechanical energy deployed by vehicles that are using the road. Hence, the primary source of the energy is provided by the users, who contribute to generating the energy that the infrastructure requires to offer them mobility. Moreover, piezoelectric harvesting is mostly independent from environmental conditions, which is a great advantage with respect to climate-dependent harvesting; its installation embedded into road pavement assures the required protection against vandalistic actions. The result is a resilient, responsible and local energy production system.

Regarding the potential applications of piezoelectric energy harvesting, according to US government information (CIA 2021), there were approximately 22 million km of paved roads worldwide in 2021. However, there are a great variety of harvesting alternatives proposed in the literature, and their associated effectiveness is still controversial. It is possible to find energy production values of approximately 1  $\mu\text{J}/\text{wheel}$ , as in the study presented by Chen et al. (2016), for different piezoelectric solutions, such as films or stacked disks. However, other authors increase this production to 400 mJ/wheel, such as in the research conducted by Sun et al. (2015) on PZT vibrating devices or the research carried out by Kok et al. (2016) on

---

✉ Ernest Bernat-Maso  
ernest.bernat@upc.edu

<sup>1</sup> Strength of Materials and Structural Engineering Department, Universitat Politècnica de Catalunya, C/Colom 11, TR45, D131, 08222 Terrassa, Spain

cymbal elements. Despite these promising results, there are still overly optimistic proposals that do not consider real traffic incidences (cars are not exciting harvesters continuously) or the significant stiffness difference between the harvester and the pavement that reduces mechanical–mechanical energy transmission efficiency. Thus, performing comprehensive research on the electromechanical characterisation of piezoelectric elements, the assessment of the embedded harvesting units in realistic conditions, and the design and optimisation of the harvesting unit, is currently the required approach to present properly contextualised data.

Considering different architectures for harvester design, there are some significant reviews focused on piezoelectric working mode alternatives, such as the study by Calìo et al. (2014), or oriented to the piezoelectric architecture for the specific application as a road pavement harvester, such as the study by Zhao et al. (2012). Concerning the piezoelectric working mode, most of the studies carried out have been based on compression-activated or bending-activated modes.

The multilayer configuration (Fig. 1) is based on stacked compression-activated piezoelectric elements that use the traffic-induced mechanical stress in pavement to generate an electrical output. The main characteristic of this configuration is the elevated stiffness (Zhao et al. 2012), which turns into a high conversion ratio; however, some authors note that the total energy harvested is reduced because a small part of the external mechanical loading is transmitted to the stiff piezoelectric system. One example of an energy harvester designed with this working principle is the one proposed by (Wang et al. 2018), who studied the use of protective pads to assure a centred and axially oriented load application for multilayer piezoelectric devices. Eccentricities or bending efforts derived from the applied load may easily lead to piezoelectric breaking; thus, these

auxiliary elements are necessary for this piezoelectric configuration. In addition, multilayer piezoelectric devices may be obtained by co-firing or adhesive processes (Wang et al. 2019), with the latter being more reliable under high loads applied at low frequencies and thus more suitable for energy harvesting in pavements. In the same study, the authors provided data about the lifespan of this kind of piezoelectric generator. Additionally, in compression mode, there is the alternative of using spherical solid piezoelectric elements, as proposed by Guo and Lu (2019). This approach eliminates the centring and orienting load issues; however, the production of spherical-shaped piezoelectric elements has not yet been industrialised.

Similar to multilayer piezoelectric devices, cymbal, bridge or moonie devices are compression activated; nevertheless, the piezoelectric elements installed in these configurations are generated in both axial and bending configurations. Moonie, cymbal and bridge configurations are all based on the same concept. These configurations are composed of a ceramic plate that has two metal end caps bonded, one at each side, leaving cavities, as shown in Fig. 1. When activated by a compressive load, the end cap transforms the axial load into a radial load, and the magnitude of this load is increased. As a result, the piezoelectric plate is generated by axial and bending modes, increasing the effectiveness of the mechanical–electrical conversion, as reported by Pérez-Lepe et al. (2016). These systems show an apparent stiffness that can be adjusted to the pavement system, allowing almost perfect mechanical compatibility with the installation environment. Among these systems, the bridge system (rectangular ceramic) seems to be the most efficient according to Zhao et al. (2012). Several applications of this end-cap auxiliary setup are found in the literature. Goh et al. (2017) proposed an asymmetric cymbal configuration to enhance its performance. Jasim et al. (2018) proposed an energy harvester

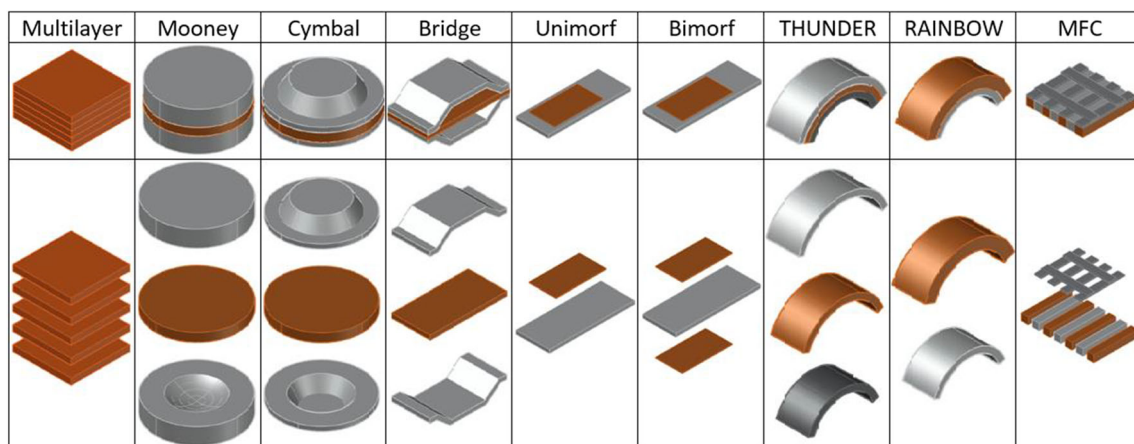


Fig. 1 Piezoelectric configurations for energy harvesting purposes

based on piling bridge units in a matrix manner to configure an energy harvester system (Fig. 2).

Alternatively, there are piezoelectric configurations based only on bending activation. This basis is the case for unimorph, bimorph, thunder, rainbow or MFC (macro-fibre composite) systems (their geometric configurations in Fig. 1). The main idea of each of these systems is to harvest energy from a mechanical vibration input. Hence, being able to modulate the mechanical vibration acting on the generator is crucial for the efficiency of these configurations. The study by Yildirim et al. (2017) notes several strategies for this task: increasing the action on the piezoelectric by adapting the shape (trapezoidal) of the plate where the piezoelectric is mounted, increasing the vibration duration by adding masses or magnetic fields, increasing the vibration amplitude by adding mechanical elements, increasing or tuning the vibration frequency by prestressing elements, defining nonlinear systems to extend the optimum frequency conversion value to a wider range, or increasing the degree of freedom of the mechanical system where bending piezoelectric devices are included to harvest energy from different types of vibration.

Hundreds of energy harvester architectures based on bending piezoelectric are available in the literature. In this paper, some of these studies are reported to illustrate the main conceptual strategies. Mitcheson et al. (2004) proposed three different designs from a simple membrane bending system to a Coulomb-force parametric generator, including a case with several degrees of freedom. Moon et al. (2014) used a radial array of cantilever plates with bending piezoelectric mounted on them that were activated by a rotational element (Fig. 2). Yang et al. (2017) proposed mounting bending piezoelectric devices on fixed-fixed plates that were simultaneously activated by an out-of-plane oscillation displacement of one of the fixed plate endings (Fig. 2). Finally, Saxena et al. (2017) proposed a system based on a 4-beam cross-shaped configuration that

had a weight in the centre as the optimum bending system for bending piezoelectric generation.

Apart from single piezoelectric transducer-type harvesters, there are alternative hybrid systems that are intended to excite different piezoelectric elements that work in different modes in a single harvester configuration. This is the case, for example, of the work presented by Xu et al. (2018), who combined bending piezoelectric elements with compression piezoelectric elements in a unique generator unit to harvest both stress-associated energy and vibration-associated energy.

To complement the possible cases, there are some energy harvesting devices that are based on secondary deformation modes to collect energy from the environment. This basis is the case for the work presented by Calìo et al. (2014), who included the study of the shear mode generator. The main issue of this alternative is that both stress and polarisation are perpendicular to the electrical output, requiring two independent sets of electrodes: one for polarisation during production of the piezoelectric and the other for the operation.

Finally, note that there are several available studies that compare different generating strategies using piezoelectrics. Among these studies, the works by Yang et al. (2017) and Xu et al. (2018) are outlined because of their wide ranges of applications considered in the energy harvesting field.

Regarding the position of the piezoelectric harvesters, they can be installed in a device embedded into the pavement or in a device apart from the pavement, leaving only the mechanical energy caption device in the road. In the latter case, the energy harvester architecture is not influenced by road pavement properties and is slightly influenced by traffic definition. In contrast, the architecture of the energy harvester and the definition of its installation position are highly influenced by several parameters in the former case. These parameters include traffic definition (weight, distance between wheels, tire footprint and speed)

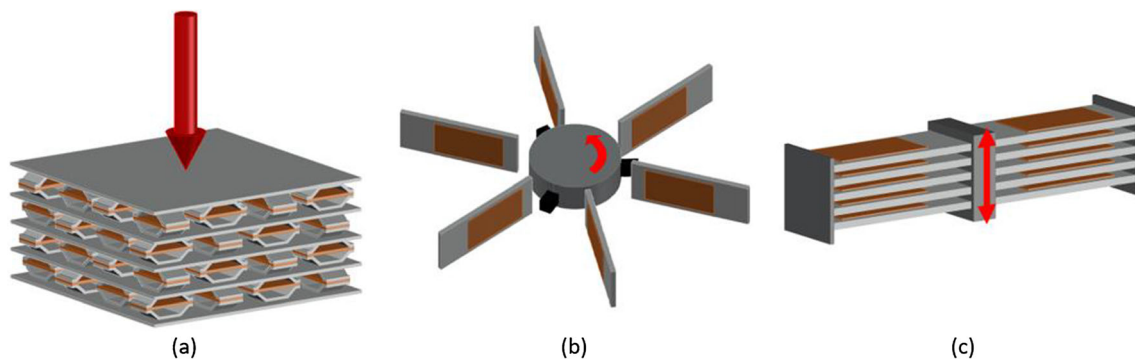


**Fig. 2** Energy harvester architecture examples. **a** Matrix array of piezoelectric bridge devices for harvesting compressive forces. Based on the concept by Jasim et al. (2018). **b** Free vibration of bending uni/bimorph piezoelectric devices activated by rotatory movement. Based

on the concept by Moon et al. (2014). **c** Forced synchronised vibration of uni/bimorph piezoelectric devices activated by oscillatory movement. Based on the concept by Yang et al. (2017)

and pavement definition (stiffness and in-depth stress diffusion). Wang et al. (2018) determined the optimal device transversal and longitudinal dimensions based on the characteristics of the tire footprint of heavy and light traffic. Additionally, the longitudinal separation between devices is calculated for light and heavy traffic based on the wheelbase. These calculations are based on the hypothesis of the superficial installation of the energy harvester and tire footprint. In contrast, Zhao et al. (2012) used the stress distribution to calculate the activation time for each wheel passing the pavement at a fixed speed. This approach allows us to characterise the expected loading pattern: activation time, frequency and load (resulting from vehicle weight estimation), which is useful for defining the loading for representative laboratory characterisation tests in a more accurate manner.

Pérez-Lepe et al. (2016) adapted the materials, geometry and structural configuration of the energy harvester to approximate the equivalent resulting stiffness of the device with the pavement to maximise the production of cymbal harvesters.

Considering the state of the art, a reasonable design for a harvesting system based on the known limitations of this technology instead of trying to reproduce optimum laboratory results in practical applications is needed. Thus, choosing low-cost membrane piezoelectric patches in a justified manner, developing an ad hoc activation system and assessing its performance under realistic conditions are the three main aims of this research. Using membrane piezoelectric elements in cymbal-like harvesters, including a punctual activation tool, is the main novelty of this research in terms of harvester design.

## 2 Materials and methods

Three types of piezoelectric elements were initially selected to perform an experimental comparison analysis of the compressive, bending and membrane alternative typologies. Based on the obtained results presented later in this study and in the literature, membrane piezoelectric patches were selected, and ad hoc harvesting encapsulation was designed and optimised by combining both experimental and finite element analysis methods. In addition, the optimal position of the harvester in standardised pavements was numerically studied. Finally, a series of 25 harvesting devices were produced and tested in three environments: isolated, embedded in a specific resin-based pavement pad and as part of a mesh of harvesting elements embedded in the analogous conditions.

The three types of piezoelectric elements that were initially considered are compressive piezoelectric ceramic disks (PRYY + 0170 by PICeramics (PI 2019)),

piezoelectric circular membranes TXJ-055-EU by Timestl (Amazon 2022) and piezoelectric bending patches DurACT P876-A12 (PI 2022).

Tests were performed to precisely determine the input mechanical action and the output electrical signal of the different piezoelectric alternatives to compare their performance levels under a loading configuration that represented the traffic action in terms of stress (maximum 1 MPa) and duration/frequency (approximately 10 Hz).

Compressive disks were tested under a theoretical cyclic action of  $\pm 314$  N range (corresponding to 1 MPa stress) at six different frequencies: 0.5, 1, 2, 4, 8 and 16 Hz. An M30 steel bar was used to apply the load (Fig. 3). Electrical resistance at the output was tuned at 398 k $\Omega$  to maximise the electrical energy harvested. Tests were repeated twice with and without a 1 mm thick neoprene plate at each side of the piezoelectric disk. These rubber pads were used to prevent the fragile breaking of the piezoelectric ceramic.

The tests on compressive piezoelectric disks resulted in production between 0.30  $\mu\text{J}/\text{cycle}$  and 5.50  $\mu\text{J}/\text{cycle}$ , depending on the testing frequency. Only the results of the tests including neoprene plates were useful, as long as piezoelectric ceramic disks broke in all cases tested without this element. Table 1 shows the testing frequency, the total force amplitude that was measured, the produced electric energy per cycle and the experimental amplitude of the displacement. Two main ideas arose from the analysis of these results. First, the energy production increased with increasing frequency of the applied load. Second, the measured displacement was under 400  $\mu\text{m}$ , including the deformation of two neoprene layers with 1 mm thicknesses. The elastic modulus of neoprene was experimentally determined for the considered stress range, and it was 9.58 MPa. This result suggested that 209  $\mu\text{m}$  was directly associated with neoprene, resulting in deformations of the ceramic disk of approximately 200  $\mu\text{m}$  or less.

Membrane piezoelectric patches were tested in a circular fixed contour configuration by applying a controlled displacement at the centre (an M6 nut was used as the loading tool). Tests were carried out with 550 k $\Omega$  electrical resistance connected at the piezoelectric output. This electrical resistance was tuned with previous tests. Testing frequencies ranged from 0.1–10 Hz. The displacement at the central point of the piezoelectric membrane patch was measured with an LVDT sensor (Fig. 4). This test setup was used for two different series. The first series applied a theoretical displacement with a fixed range of 70  $\mu\text{m}$ , and the frequency was modified. The second series was performed at a fixed frequency of 4 Hz, and the applied displacement amplitude was modified. These two different series were set because the data from the first series were

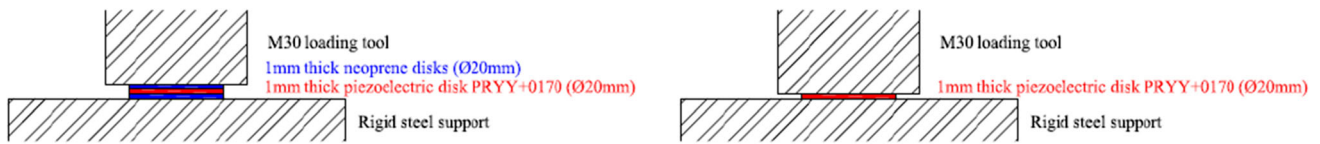


**Fig. 3** Test setup for compressive piezoelectric disks with neoprene contacting the disk (left) and without neoprene contacting the disk (right)

**Table 1** Results of the characterisation tests on piezoelectric compressive disks

f (Hz)	F(N)	E <sub>OUT</sub> (μJ/cycle)	a(μm)
0.5	604	0.30	407
1	596	0.53	382
2	598	1.04	359
4	616	2.24	358
8	610	3.54	338
16	566	5.50	291

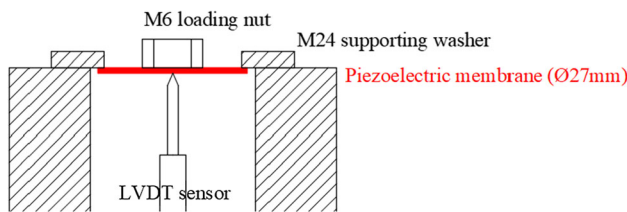


**Fig. 4** Test setup for membrane piezoelectric patches

used to calibrate the numerical model, whereas the second series was used to validate it with an independent dataset.

By observing the results of the tests on piezoelectric membrane patches of the first series (Table 2), the electrical output energy was found to range from 0.28 μJ/cycle–4.72 μJ/cycle, depending on the excitation frequency. However, in this case, it seemed that the optimum results were obtained at an excitation frequency of 6 Hz, being less efficient for higher frequencies. The measured applied

**Table 2** Results of the characterisation tests on piezoelectric membrane patches when imposing a theoretical fixed displacement of 70 μm

f (Hz)	F (N)	E <sub>OUT</sub> (μJ/cycle)	a (μm)
0.1	32	0.28	70
0.5	30	1.17	62
1	29	1.75	58
2	26	2.11	47
4	27	4.43	48
6	26	4.72	47
8	24	3.99	36
10	26	3.35	42

force corresponded to an approximate equivalent stress of 2.5 MPa on the M6 nut effective surface, which was only 0.3 MPa if the surface of the ceramic was considered. These results were used later to calibrate the numerical model.

The results of the second characterisation series of membrane piezoelectric patches are summarised in the first two columns of Table 3 and Figure. 5. For a fixed excitation frequency, increasing the movement amplitude caused an increase in the output energy that exceeded 10 μJ/cycle. These results were used later to validate the numerical model.

Finally, bending piezoelectric patches were tested after mounting them on cantilever beams. Six different beams, including two materials (polystyrene and aluminium) and three lengths, were used. The beams were excited with a cyclic displacement of a fixed range and by varying the frequency from 2–20 Hz. The optimum electrical output load was set at 230 kΩ after tuning. An extensive report about these tests is in (Bernat-Maso and Mercedes 2022). The best results of these tests were obtained when piezoelectric devices were mounted on aluminium plates. In this case, the produced energy moved from 96 μJ/cycle–957 μJ/cycle in the cases of 5 mm displacement imposed at 7.9 Hz and 10 mm displacement imposed at 21.7 Hz, respectively.

By comparing the overall performance levels of the three tested piezoelectric elements, it was possible to select the optimum one for the intended research. First, membrane and compressive piezoelectric devices obtained

**Table 3** Results of the validation simulations of numerically modelling the piezoelectric response

a(μm)	E <sub>OUT_EXP</sub> (μJ/cycle)	E <sub>OUT_SIM</sub> (μJ/cycle)	Variation (%)
16	0.67	0.30	−55.2
21	0.25	0.52	108.0
29	1.67	0.99	−40.7
44	2.88	2.29	−20.5
60	5.05	4.25	−15.8
75	6.29	6.64	5.6
87	7.17	8.94	24.7
98	11.36	11.34	−0.2
105	10.50	13.02	24.0



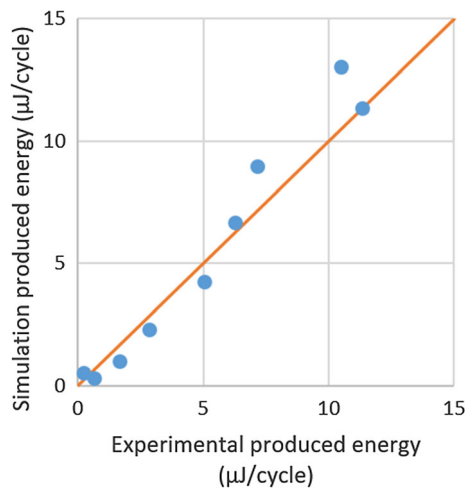


**Fig. 5** Test setup for membrane piezoelectric patches

similar output energies per cycle; however, the second device showed fragile behaviour, resulting in a nonreliable alternative requiring complex load distribution systems, such as those presented by Wang et al. (2018). In addition, the cost of the compressive disk was approximately 10 €, whereas it was 0.50 € for the membrane piezoelectric patch. Thus, between these two alternatives, a membrane piezoelectric patch would be selected. Compared with the bending patch, this last patch produced far more energy (approximately 200 times more than the membrane piezoelectric patch); however, it required large deformations (over 5 mm) that were incompatible with embedding them into the pavement. In addition, bending patches cost approximately 65 €, resulting in an equivalent cost per unit of produced energy to the membrane piezoelectric patches. Thus, because of their mechanical compatibility with the required application, their robustness and their reduced cost, membrane piezoelectric patches were selected to carry out the development of the energy harvester.

The harvesting device was designed using finite element analysis tools. The general-purpose software ANSYS Workbench™ R19.2 was used. The realistic geometry of the piezoelectric was considered, including the brass plate (27 mm diameter and 0.2 mm thick) under a piezoelectric ceramic (17.5 mm diameter and 0.01 mm thick); however, the adhesive between these two materials was neglected. The initial piezoelectric properties were assumed to be those from the PIC255 ceramic (PI 2023) ( $d_{31a} = 194.7$  pC/N). This property was included in a similar manner to (Mehrabi et al. 2019). The first simulations aimed to calibrate the piezoelectric responses of the selected membrane piezoelectric patches. This first model represented the characterisation test in Fig. 4. 2D axisymmetric simplification was considered. The external contour of the brass plate was fixed, whereas an imposed displacement was

applied perpendicular to the membrane piezoelectric patch plane at its centre. Different values of imposed displacement were considered corresponding to the experimental evidence. All parts were completely bonded on their contacts. Mesh convergence analysis was carried out, resulting in discretisation of the domain of the harvester into elements of different sizes depending on the required accuracy and computational resources. Piezoelectric ceramic was discretised into 2 µm size elements, whereas the rest of the parts used a larger size of 50 µm. The total number of finite elements of a representative studied harvester was 35000. A total of 21000 of these elements were aimed at discretizing the piezoelectric part, and 20,000 of them represented the piezoelectric ceramic. In all cases, these elements were PLANE183 type, which are 8-node quadratic displacement elements.

The obtained results are summarised in Table 3, where  $a$  is the imposed displacement, the second and third columns are the electrical output energy per cycle (experimental and simulated) and the last column shows the relative difference between these two values. The average of the absolute values of the relative error between the simulation and experimental results was 32.7%. This error was 14% if the five cases with higher produced energy were considered. Figure 5 presents these results graphically, and good accuracy could be noticed. Thus, modelling of the piezoelectric response was accurate enough for use as a reference to develop the energy harvester device.

After characterising and validating the model of the membrane piezoelectric patch, the design of the harvester unit was based on numerical simulations to optimise the mechanical definitions of two cymbal plates. 2D axisymmetric hypotheses were considered in the optimisation of the harvesting device. The optimisation procedure included hundreds of simulations modifying the bottom and top diameters, height, thickness, bending radius of the cymbal plate, the thickness of the neoprene washers and the presence/absence and radius of the inner contacting tool. In addition, this inner contact column was initially set as an empty cylinder defined by its internal and external radii. Including this inner contacting column (Fig. 6) is a novelty of this research that the authors have not found in the literature. Optimising this element was a key point of the methodology. Each variable was modified independently of the others to look for the associated trend.

All parts were bonded, and PLANE183 elements were used. Mesh convergence analysis was carried out, resulting in discretisation of the domain in 2 µm size elements for piezoelectric and 50 µm size elements for the rest of the parts. The optimisation process sought to maximise the average strains in piezoelectric ceramic but limited them to a maximum value of 0.00175 (Guillon et al. 2004) to prevent fragile breaking. In addition, a safety factor of 1.5

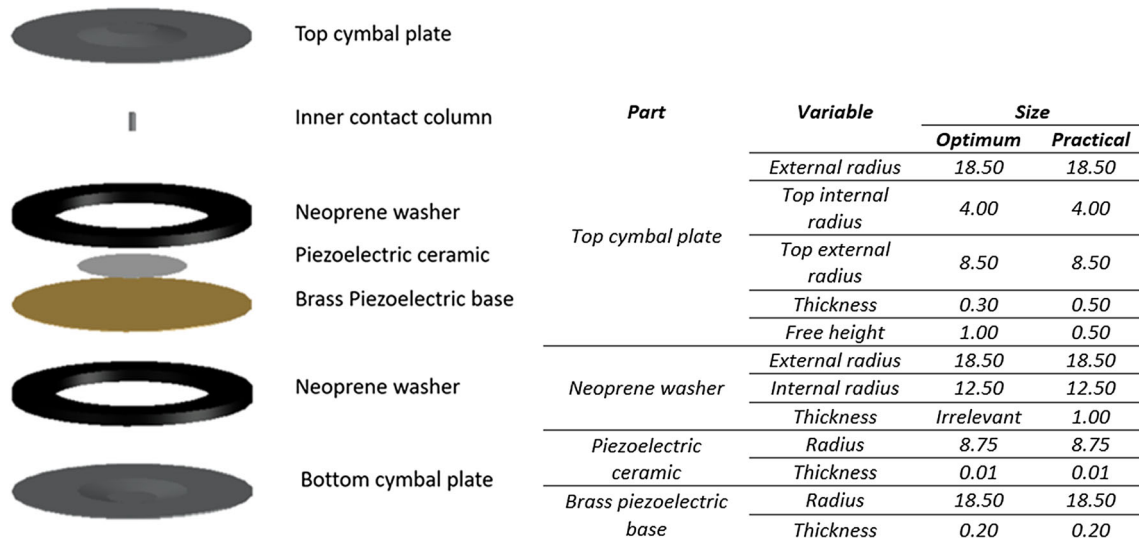


Fig. 6 Optimum and practical designs of the harvesting device. Units in mm

was set on the von Mises equivalent stress value in comparison with the yielding stress for cymbal aluminium plates (260 MPa). Aluminium was set for the inner contact column.

The optimisation process was iterative because adjusting one of these variables affected the optimum values of the other variables. Thus, the initial sensitivity analysis was presented (Fig. 7) to illustrate the trends of all these variables. The average strain in the piezoelectric ceramic was used as a comparative variable because the generated energy was directly related to it. Using the strain to carry out the optimisation of the harvester made it possible to analyse the mechanical problem without including the piezoelectric effect to reduce computational cost. Figure 7a shows that including the inner contact column increased the produced energy by approximately ten times, and it was beneficial for reducing the thickness of the cymbal. Regarding the geometry of the inner contact column (Fig. 7b), reducing the external radius caused significantly increased the produced energy; reducing the internal radius (Fig. 7c) increased the generated energy. Regarding the internal and external radii of the cymbal (Fig. 7d and e), increasing both was associated with an increase in the generated energy, although modifying the external radius showed a greater effect. With the opposite trend, reducing the free height of the cymbal (Fig. 7f) increased the output electrical energy.

Modifying the thickness of the neoprene washer had no effect according to the simulation results. The optimum design was the one presented in Fig. 6 with a solid inner contact column of 1 mm radius.

Regarding the study of the influence of the position of the harvesting device on standardised pavement configurations, two asphaltic pavement standard definitions (4211

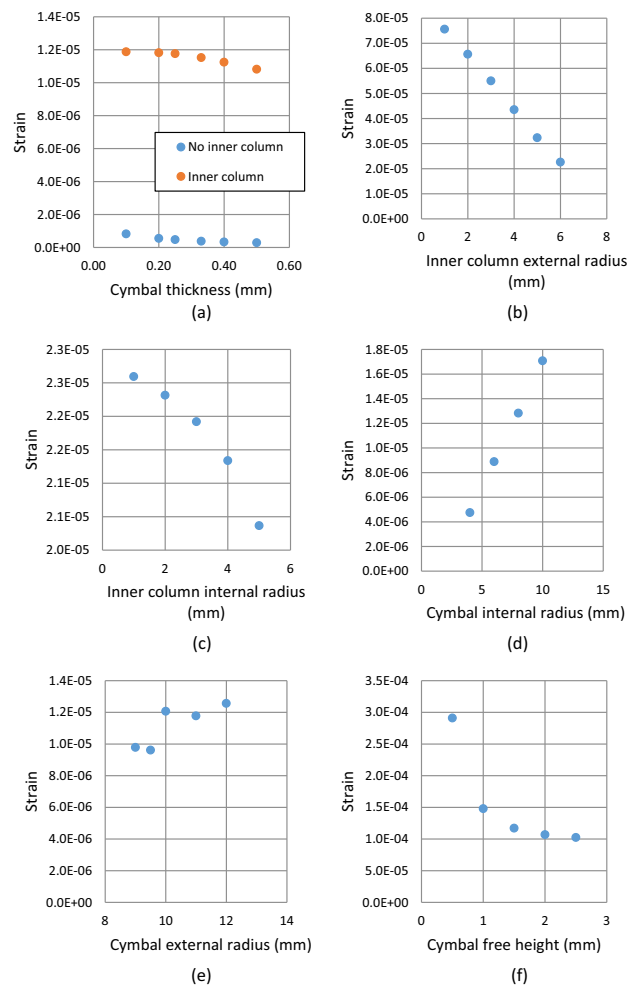


Fig. 7 Sensitivity analysis of the variables defining the design of the harvester

flexible and 0032 stiff according to 27, see Fig. 8 for material properties of the pavement) and four extreme positions of the harvesting device in the top layer of the pavement were considered: (TC) centred under the load with its upper part levelled with the pavement surface, (TD) at the same height but 900 mm from the centre of the applied load, (BC) the bottom face of the harvester levelled with the interface between the top layer and the bottom layer and centred under the load, and (BD) at the same height but 900 mm from the centre of the applied load (Fig. 8c).

2D axisymmetric simulations were used to keep the coherence with previous optimisation analysis and to use smaller size elements for the discretisation of the harvester device without increasing the computational requirements over the available resources.

Different horizontal positions ( $R = 0\text{--}900\text{ mm}$ ) and vertical distances ( $D = 0.01\text{--}32.6\text{ mm}$  (0032)/ $42.5\text{ mm}$ (4211)) were simulated between cases TC, TD, BC and BD (Fig. 8). The results were plotted and are displayed in Fig. 9; the average strain in the piezoelectric ceramic was used as a comparison variable.

By analysing the effects of the horizontal position, several points between BC and BD were analysed for both pavement systems (stiffer 0032 and more flexible 4211); the results were plotted and are displayed in Fig. 9 on the left. It must be noted that the position levelling the bottom face of the harvester to the interface between the top pavement layer and the following one was different for the 0032 definition (32.6 mm) than for the 4211 configuration (42.5 mm). Nevertheless, the trend was the same: the greater the distance between the load and the position of the harvester, the lower the deformation obtained in the

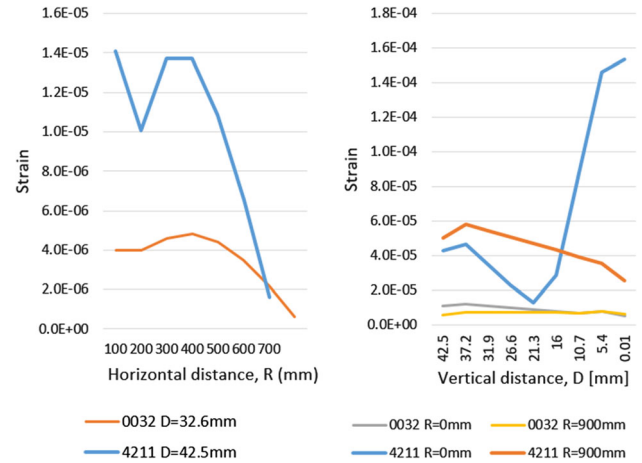
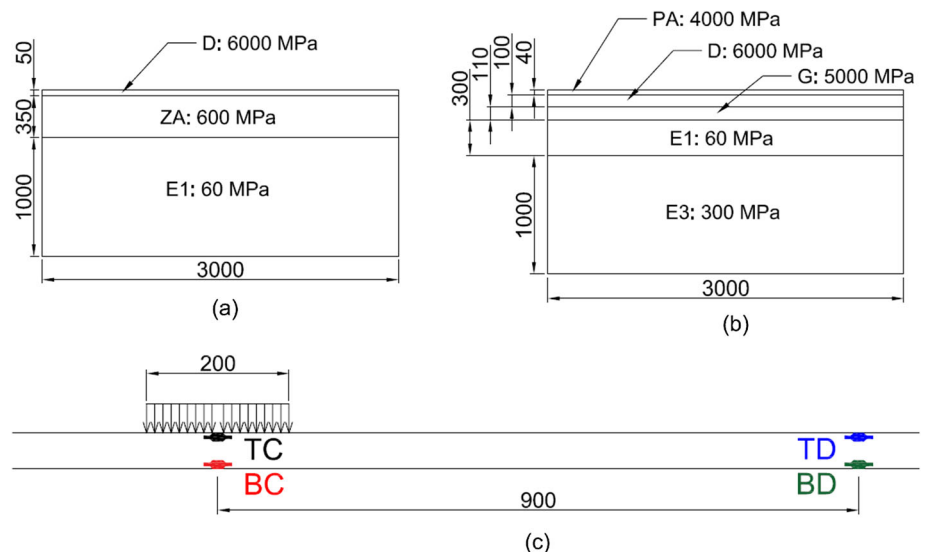


Fig. 9 Numerical results of the optimisation of the harvester position in the pavement. Horizontal position (left) and vertical position (right)

piezoelectric body. The beginnings of these curves were altered by the 200 mm definition of the load radius. For all positions, using a more flexible solution allowed a greater (over three times) strain inside the piezoelectric unit. Regarding the effect of the in-depth position of the harvester, for all cases, the strain decreased when the harvester was closer to the surface. This phenomenon could be due to the beneficial effect of the harvester being surrounded by the more flexible environment (2nd pavement layer). However, this finding was not the case for the centred position under the load in 4211 pavement, which showed greater strains when the harvester was immediately placed under the load at the pavement surface.

Fig. 8 a 4211 pavement definition. Dimensions in mm. b 0032 pavement definition. Dimensions in mm. c Studied positions of the harvesting unit with respect to the road path: TC stands for top centred, TD stands for top displaced, BC stands for bottom centred and BD stands for bottom displaced. Dimensions in mm





**Table 4** Results of the tests on isolated harvesters

Inner contact column	Neoprene washer thickness (mm)	Force range (N)	$E_{OUT}$ (J/cycle)
4 mm wood cube	5	113	$6.98 \cdot 10^{-8}$
2 M2 nylon nuts	5	113	$1.01 \cdot 10^{-7}$
M2 stainless steel nut	1	113	$1.08 \cdot 10^{-7}$
2 M4 stainless steel washers	1	113	$1.19 \cdot 10^{-7}$
No inner contact column	1	113	$7.01 \cdot 10^{-9}$

**Fig. 10** (left) Sketch of the 4 considered embedding positions of piezoelectric harvesters into Firflex™ resin and (right) pad with a single embedded harvester (case of embedding type 2)

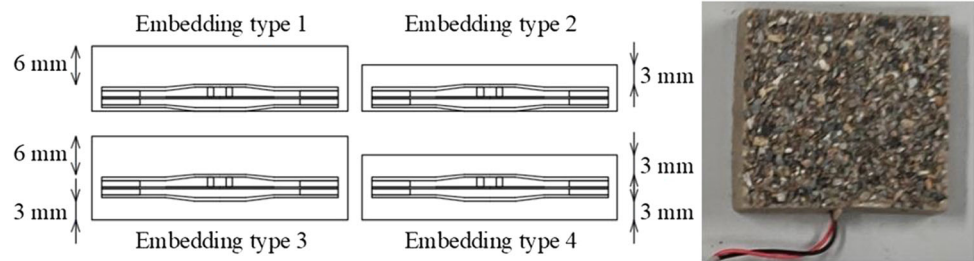


**Table 5** Tests and results of single embedded harvesters

Test	$E_{OUT}$ single (J/cycle)	Embedding type	Testing orientation	$E_{OUT}$ embedded (J/cycle)	Difference (%)
11U-1	2.60E-8	1	Upwards	9.66E-8	272
11U-2		1	Upwards	8.54E-8	228
12U-1	4.72E-8	1	Upwards	8.98E-10	-98
12U-2		1	Upwards	1.22E-9	-97
12D-1		1	Downwards	1.19E-9	-97
21U-1	5.77E-8	2	Upwards	7.80E-9	-86
22U-1	1.98E-9	2	Upwards	1.24E-9	-37
22U-2		2	Upwards	9.06E-10	-54
31U-1	6.31E-8	3	Upwards	9.01E-10	-96
32U-1	5.95E-8	3	Upwards	5.62E-8	-5
32D-1		3	Downwards	5.71E-8	-4
41U-1	1.63E-8	4	Upwards	2.93E-9	-82
42U-1	1.59E-8	4	Upwards	1.35E-10	-99
42D-1		4	Downwards	2.11E-9	-87

### 3 Experimental tests on harvesters, results and discussion

To validate the theoretical design, several tests were conducted on insulated harvesters, single embedded harvesters and a grid of interconnected harvesters. First, to produce the proposed energy harvesters, aluminium sheets of 0.5 mm thickness were used to produce cymbal plates to embed the selected membrane piezoelectric patches. A 1 and 5 mm thick neoprene rubber was used for the electrical isolation of the piezoelectric part and to promote its deformation, although theoretical results showed no influence. To extend the experimental study of alternative designs of the harvester, a stainless steel M2 nut, two

stainless steel M4 washers, an M2 nylon nut or 4 mm edge wood cubes were mounted between the top cymbal plate and the piezoelectric membrane patch in such a manner that it was partially prestressed, and the load transmission was punctually applied on the centre of the piezoelectric membrane patch to maximise its deformation. Finally, harvesters were embedded into a flexible resin typically used for punctual road repair (Firflex™ by Sorigué). This alternative provided a more flexible environment (favourable with previous simulation results), and it assured high bonding performance to place the devices closer to the surface exposed to the traffic action. Firflex™ is a mixture of polymers and alcohols, and its main component is methyl methacrylate.

First, cyclic compressive tests on different single harvester units were carried out to experimentally assess the influences of some of the practical design variables (inner contact column definition and thickness of neoprene washer) on the electrical output. The mechanical action was constant, and it was defined as a cyclic load with a 1 MPa range and a 10 Hz frequency. Load cycles were implemented to maintain a minimum compressive stress of 0.1 MPa during the tests; thus, there was an average compressive stress of 0.6 MPa (action was  $0.6 \text{ MPa} \pm 0.5 \text{ MPa}$ ). This load definition was aimed at preventing the movement of the harvesters that were simply laid on a plain steel surface tooling. The load was directly applied on the top cymbal surface.

The applied force and displacement, with the output voltage signal at an electrical resistance of 550 k $\Omega$ , were simultaneously recorded at 50 Hz. Table 4 shows a summary of the results of the tests.

According to the empirical results, including the inner contact column increased the generated energy over 10 times when comparing the wood cube case with the case with no inner contact column. This difference was even larger when compared with the other tested cases. Because of the lower stiffness of the wood with respect to the nylon nuts, lower energy was generated for the former. By analysing the influence of the thickness of the neoprene washer, it was clear that there was not a significant effect if the inner contact column completely covered the free height between the piezoelectric ceramic and the intrados of the top cymbal plate. Thus, this result supported the evidence that was numerically obtained. Finally, by comparing the two alternatives with stainless steel inner contact elements, there was not such a significant difference; nevertheless, it was far easier to produce the harvester with one M2 nut than piling two M4 washers. However, according to the numerical results, it was expected that the M2 nut alternative produced more energy than the M4 washers because the former had a smaller contact area. This difference could be because two M4 washers (0.8 mm thickness each) including an additional glue layer could

have reached a greater height than a single M2 nut (1.6 mm), causing a beneficial prestress of the piezoelectric ceramic that could help electrical production but limit the available strain range for operation.

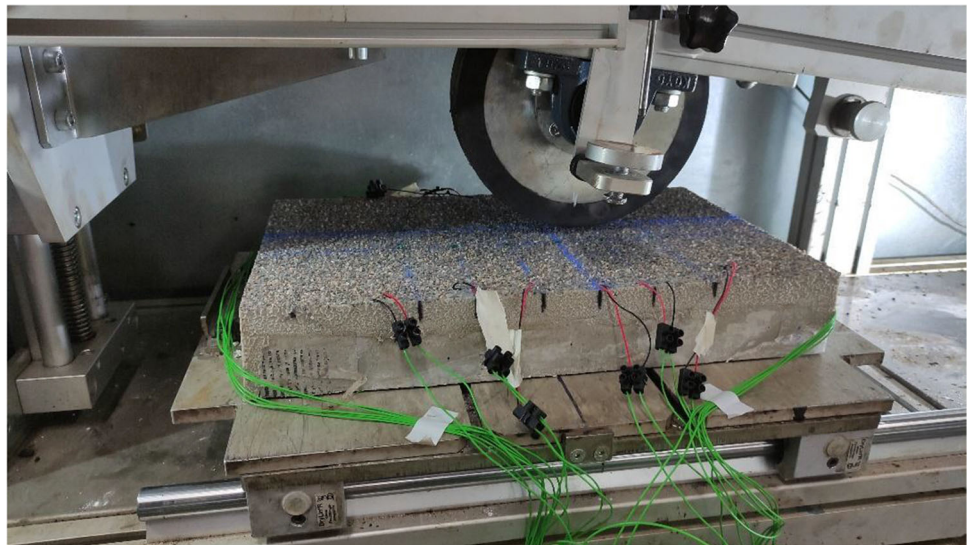
Moving to the tests on single harvesters embedded into a resin pad, only the practical design of the harvester reported in Fig. 6 was used according to the results of the tests on insulated harvesters. Eight units of the practical harvester design (Fig. 6, with the M2 nut as the inner contact column) were embedded into 4 different types of individual resin pads (2 repetitions per case), and these were tested under the same loading conditions as the tests on insulated harvesters. The only difference was that the load application surface corresponded to the footprint of a steel loading tool 42 mm in diameter in this case. A neoprene disk of 3 mm thickness was placed between the loading tool and the specimen to avoid punctual stress concentrations and to represent real tire action in a more approximate manner. Tests considered four different positions of the harvester in the resin pad: the bottom face of the harvester levelled with the bottom face of the resin pad and 3 or 6 mm of resin covering on the top and two more configurations with the same definition of top coverings but considering 3 mm of bottom resin covering. All of them were covered with sand particles in the top surface to assure the grip with the tires in the intended future practical use. A sketch of the specimens and the corresponding test setup is presented in Fig. 10.

The results are summarised in Table 5, including the test labelling in the first column, the energy per cycle generated by the same harvesting unit when insulated, the type of embedding according to Fig. 10, the energy per cycle generated after embedding the harvester into the individual resin pad and the relative difference in percentage with respect to the nonembedded unit. The test labelling configuration was in the form XYA-R, where X stands for the type of embedding, Y stands for the sample of the series with the same embedding type (two samples per series), A stands for the upwards (U) or downwards (D) direction and R stands for the repetition of the same test. Only some

**Table 6** Tests and results of multiple embedded harvesters

Test	Wheel position	Speed (cycles/min)	Connection	Temperature ( $^{\circ}\text{C}$ )	Energy 1 cycle 1 unit (J)
L1-M-I-25	L1	26.5	Independent	25	8.93E-10
L1-H-I-25	L1	32.4	Independent	25	1.57E-10
L2-M-I-25	L2	26.5	Independent	25	2.17E-9
C-M-I-25	C	26.5	Independent	25	8.23E-10
C-M-S-25	C	26.5	Series	25	5.26E-13
C-M-S-60	C	26.5	Series	60	6.03E-13

**Fig. 11** Wheel-tracking test on a pad with 12 piezoelectric harvesters



initial tests were repeated to assure repeatability of the testing method.

First, the repeatability of the testing methodology was assessed. By comparing the results of the two repetitions of the tests 11, 12 and 22U (Table 5), an average coefficient of variation of 17.4% was obtained. Although this average difference was significant, it was low enough to find trends of the results from different cases. In addition, due to the different performance of each individual unit because of manual fabrication, it was preferred to perform individual comparisons to assess the effects of embedding harvesters.

By focusing on particular results, it was surprising that the first type of embedding tested in the upwards direction obtained approximately three times more energy per cycle than the insulated harvester for the first repetition of the test. This result contradicted the tendency of all the rest of the tests. Therefore, these results were neglected from this analysis.

By comparing the four embedding typologies, it was clear that the most effective one at limiting the losses of electric generation capacity was that consisting of 6 mm of top covering and 3 mm of bottom covering. This fact supported the idea of the benefits of embedding piezoelectric harvester units into the most flexible environment possible for the specified technology that benefitted from large deformations. Thus, it was concluded that the effectiveness of the proposed harvesting units would increase when embedded into flexible environments close to the surface of traffic action. This evidence was completely supported by the numerical results that indicated that surrounding the harvester with flexible pavement would be beneficial for mechanical strain amplification and energy production. Because of this, the selection of Firflex<sup>TM</sup> resin was completely justified by the obtained results.

Finally, a mesh of 12 (2 lines of 6 harvesters each) piezoelectric harvesters defined according to the practical design (Fig. 6, with M2 nut as inner contact column) was embedded into a resin pad in the best position (embedding type 3, 6 mm of resin covering at the top and 3 mm of resin covering at the bottom, as per Table 5) according to the results of the previous tests on insulated embedded harvesters. This resin pad, including the piezoelectric harvesters, was built on a high strength mortar element of 250 mm × 120 mm × 40 mm to obtain the required dimensions of the sample to perform the test. The load was applied with a wheel-tracking test (EN-12697) setup to simulate realistic traffic action. Three positions of the wheel were tested: over one line (L1), over the other line (L2) and centred (C) between them. Two testing speeds were considered. Electrical output was measured independently and connecting harvesters in series. The sample was tested under high environmental temperature (60 °C). In all cases, the pressure was 1 MPa. The combination of these testing variables is shown in Table 6. Figure 11 shows a picture of the testing setup.

The electrical output terminals of every piezoelectric harvester were connected to a standard interface conditioning circuit consisting of a diode bridge in parallel to the optimum load resistance (560 kΩ) and a capacitor of 470 μF. The voltage was measured between the terminals of the electrical resistance at 50 Hz. For some of the tests, the electrical signal was independently measured for every piezoelectric harvester, and for other tests, the output signal was measured after serial connection of the outputs of every conditioning circuit. In the first case, the average of the produced energy per activation and unit was calculated as the comparison result. In the second case, the total energy produced per cycle was divided by the number of harvesting units (12) to obtain comparable data. The results

were summarised and are displayed in Table 6, showing the electrical energy produced at the output of the conditioning circuit per activation cycle and per piezoelectric harvester unit.

After observing the results, the first comment was that any of the average values of the produced energy were close to those obtained in the 11U tests. Thus, this additional checking supported the idea of discarding 11U results from the previous discussion. Moreover, the maximum individual production measured during all tests on piezoelectric grids was  $3\text{E-}8$  J per cycle and harvester, which was in the range of 12U tests, supporting the previous comment.

By comparing the previous results with these results, including the standard interface conditioning circuit did not cause a significant loss in the produced energy, which moved from  $1.10\text{E-}9$  J (average of 12U cases) to  $1.07\text{E-}9$  (average of L1 and L2 cases), indicating a reduction of 2.6%.

By comparing the average energy produced by the harvesters when directly activated by a load centred on them (L1-M-I-25 and L2-M-I-25 cases,  $1.53\text{E-}9$  J) with the comparable case with a load centred between the lines of harvesters (C-M-I-25,  $8.23\text{E-}10$ ), an increase over 85% was recorded when the load was directly applied on the units relative to the case in which the load was 30 mm apart. This point highlighted the importance of installing harvester units in the most likely footprint line of the traffic.

Regarding the testing conditions, increasing the testing speed by approximately 20% (from 26.5 cycles/minute to 32.4 cycles/minute) was not translated into an energy production increase. In fact, the energy production was reduced to approximately a sixth part. Nevertheless, individual measurements of tests L1, L2 and C-M-I-25 were useful for detecting that the harvester unit that always produced more energy was placed close to the centre of the wheel path where the loading/unloading speed was greater. This unit produced approximately double (maximum  $6.4\text{E-}8$  J) the average ( $1.53\text{E-}9$  J for the L1-M and L2-M cases). Thus, this evidence was in line with other studies that noted the dependency of the energy produced on the activation speed or frequency (Bernat-Maso and Mercedes 2022; Damjanovic 1997; Umeda et al. 1996).

Regarding electrical connection, a reduction of three orders of magnitude of the produced energy when comparing individual production (C-M-I-25) and in series connected harvester production (C-M-S-25) indicated that local storage was required to further gather the produced energy.

Finally, the increase in temperature during testing had no significant effect on energy production; it could even be slightly beneficial because of the stiffness reduction of the media surrounding the harvesting unit.

After analysing the overall results, only  $10\text{E-}5$  of the input energy was converted into useful electrical energy. The average detected losses in the investigated system were as follows:

- 0.5% efficiency in mechanical–electrical transformation of direct tests on piezoelectric membrane patches for realistic stresses and frequencies. This finding indicated that only 1/200 of the input mechanical energy was transformed to electrical energy by this type of piezoelectric patch.
- 3% efficiency due to the inclusion of the piezoelectric membrane patch into a modified cymbal harvester to protect it from local stresses. This finding indicated that only 1/30 of the mechanical energy reached the piezoelectric membrane patch.
- 84% efficiency due to embedding harvesters into pavement in comparison to aisled harvesters, even if it was as flexible as the Firflex system.
- 100–0.1% efficiency due to electrical connection if it was only due to the standard interface conditioning circuit or if it included a series connection. Thus, in the best case of directly using the connection of the conditioning circuit, nonsignificant losses could be considered.

Thus, by considering all the possible losses of the system, a final efficiency of the task of turning mechanical energy into electrical energy of approximately 0.014% was expected with the proposed system. By comparing the different efficiencies, it was clear that the main drawbacks were the low efficiency of the selected piezoelectric membrane patches, which could be improved by selecting other materials, and the strain restrictive effect of including the piezoelectric membrane patches in the harvester units to protect them from the direct actions of traffic.

## 4 Conclusions

A comprehensive experimental campaign including direct characterisation tests of the piezoelectric elements, optimisation of the harvesting units, assessment of the effects of embedding harvesters into pavement and consideration of the effect of a realistic traffic action has been carried out. This experimental research has been complemented by numerical simulations addressing the optimisation of the harvester design and the positioning of the harvester units into the pavement. The main conclusions obtained from this research are as follows:

- Membrane piezoelectric patches are selected for road harvesting among bending patches and compressive disks because of their mechanical compatibility with the pavement. Bending patches require excessively



large deformations, and compressive disks are too stiff for this intended application.

- The implemented numerical model correctly reproduces (32.7% of average of the absolute value of the relative error and 14% in more representative cases) the piezoelectric response of the selected piezoelectric membrane patches for the applied load (stress level and frequency).
- Including the novel inner contact column increases the mechanical strain in the piezoelectric membrane patch ten times.
- The results of the optimisation during the design of the cymbal harvester indicate that future works may aim to produce more flexible harvesting devices. A specific feasible design has been obtained.
- Although the harvester is flexible enough to correctly transmit the mechanical energy to the piezoelectric membrane patch, it is necessary to embed this device into a more flexible pavement than the existing ones. In this manner, using modified resins that assure the required durability is an alternative.
- Regarding the position of the harvesters in the pavement, it is essential that units are placed under direct wheel action. However, it seems that it is not highly important to place them exposed at the surface; thus, it is possible to embed this energy production system several centimetres under the surface, preventing damages.
- From the experimental results of the wheel-tracking test, it is observed that the electric production is highly dependent (potentially doubling the production) on the system activation speed.
- The obtained performance of the designed system guides its possible future application to the supply of small sensors in the road system. Lightning applications are too demanding for the proposed low-cost system.

Finally, the main conclusion is that it is feasible to produce low-cost energy harvesters with membrane piezoelectric patches included in a cymbal configuration enhanced by the proposed novel inner contact column.

**Acknowledgements** The authors want to acknowledge the technical support provided by SORIGUÉ, S.A. through the PIEZOROAD research contract and the participation of Núria Querol and Mar Subarroca as asphalt mixture experts. The authors want to acknowledge the economic support provided by CDTI. The first author is a Serra Húnter Fellow. The second author was supported by an FPU-UPC B. Santander Universidades grant. The fourth author was supported by FPI-UPC grant 2019.

**Funding** Open Access funding provided thanks to the CRUE-CSIC agreement with Springer Nature.

**Open Access** This article is licensed under a Creative Commons Attribution 4.0 International License, which permits use, sharing,

adaptation, distribution and reproduction in any medium or format, as long as you give appropriate credit to the original author(s) and the source, provide a link to the Creative Commons licence, and indicate if changes were made. The images or other third party material in this article are included in the article's Creative Commons licence, unless indicated otherwise in a credit line to the material. If material is not included in the article's Creative Commons licence and your intended use is not permitted by statutory regulation or exceeds the permitted use, you will need to obtain permission directly from the copyright holder. To view a copy of this licence, visit <http://creativecommons.org/licenses/by/4.0/>.

**Data availability** Original raw data, data sets generated during the current study and numerical models are available from the corresponding author on reasonable request for non-commercial purposes.

## References

- Amazon TimeSTL 15pcs Accessories Pickup Bass Accessories 27mm Discos Piezoelectricos con Conductores Microfono Tambo Noiseless Pickups Dimarzio Humbucker Pickups Latón (2022) Accessed 5 Jul 2022
- Bernat-Maso E, Mercedes LE (2022) Piezoelectric elements subjected to low frequency excitation. Empirical determination of stress and frequency influence on piezoelectric parameters. *Microsyst Technol.* <https://doi.org/10.1007/s00542-022-05331-7>
- Calìo R, Rongala U, Camboni D, Milazzo M, Stefanini C, de Petris G, Oddo C (2014) Piezoelectric energy harvesting solutions. *Sensors* 14:4755–4790. <https://doi.org/10.3390/s140304755>
- Chen Y, Zhang H, Zhang Y, Li C, Yang Q, Zheng H, Lü C (2016) Mechanical energy harvesting from road pavements under vehicular load using embedded piezoelectric elements. *J Appl Mech.* <https://doi.org/10.1115/1.4033433>
- CIA. US government No Roadways—The world factbook (2021) <https://www.cia.gov/the-world-factbook/field/roadways/country-comparison>. Accessed 12 Jul 2021
- Damjanovic D (1997) Logarithmic frequency dependence of the piezoelectric effect due to pinning of ferroelectric-ferroelastic domain walls. *Phys Rev B Condens Matter Mater Phys* 55:R649–R652. <https://doi.org/10.1103/PhysRevB.55.R649>
- Fernandes JR, De Sá FA, Santos JL, Joanni E (2002) Optical fiber interferometer for measuring the d33 coefficient of piezoelectric thin films with compensation of substrata bending. *Rev Sci Instrum* 73:2073. <https://doi.org/10.1063/1.1463713>
- Goh PH, Li MJ, Tsou NT (2017) The design and analysis for low-frequency piezoelectric cymbal transducers. *Ceram Int* 43:S49–S54. <https://doi.org/10.1016/j.ceramint.2017.05.207>
- Guillon O, Thiebaud F, Delobelle P, Perreux D (2004) Tensile behavior of PZT in short and open-circuit conditions. *Mater Lett* 58:986–990. <https://doi.org/10.1016/j.matlet.2003.08.011>
- Guo L, Lu Q (2019) Numerical analysis of a new piezoelectric-based energy harvesting pavement system: lessons from laboratory-based and field-based simulations. *Appl Energy* 235:963–977. <https://doi.org/10.1016/j.apenergy.2018.11.037>
- Jasim A, Yesner G, Wang H, Safari A, Maher A, Basily B (2018) Laboratory testing and numerical simulation of piezoelectric energy harvester for roadway applications. *Appl Energy* 224:438–447. <https://doi.org/10.1016/j.apenergy.2018.05.040>
- Kok BC, Gareth S, Goh HH, Utraphan C (2016) Electromechanical-traffic model of compression-based piezoelectric energy harvesting. *MATEC Web Conf* 70:10007. <https://doi.org/10.1051/mateconf/20167010007>
- Mehrabi H, Hamed M, Aminzadeh I (2019) A novel design and fabrication of a micro-gripper for manipulation of micro-scale



- parts actuated by a bending piezoelectric. *Microsyst Technol*. <https://doi.org/10.1007/s00542-019-04696-6>
- Ministerio de Fomento (2003) Norma 6.1 IC Secciones de firme. Boletín Oficial del Estado (Spanish Official State Gazette), 12 Decembre 2003. [https://www.mitma.gob.es/recursos\\_mfom/1010100.pdf](https://www.mitma.gob.es/recursos_mfom/1010100.pdf). Accessed 6 July 2022
- Mitcheson PD, Green TC, Yeatman EM, Holmes AS (2004) Architectures for vibration-driven micropower generators. *J Microelectromechanical Syst* 13:429–440. <https://doi.org/10.1109/JMEMS.2004.830151>
- Moon JW, Jung HJ, Baek KH, Song D, Kim SB, Kim JH, Sung TH (2014) Optimal design and application of a piezoelectric energy harvesting system using multiple piezoelectric modules. *J Electroceram* 32:396–403. <https://doi.org/10.1007/s10832-014-9934-0>
- Pérez-Lepe A, Rueda SH, Izquierdo Rodríguez MA, Cuadros DU, Rubio-Marcos F, Moure A, Fernández JF, Gonzalo A (2016) Feasible integration in asphalt of piezoelectric cymbals for vibration energy harvesting. *Energy Convers Manag* 112:246–253. <https://doi.org/10.1016/j.enconman.2016.01.030>
- PI Ceramics Piezoelectric Discs (2019) [https://static.piceramic.com/fileadmin/user\\_upload/physik\\_instrumente/files/datasheets/disc-Datasheet.pdf](https://static.piceramic.com/fileadmin/user_upload/physik_instrumente/files/datasheets/disc-Datasheet.pdf). Accessed 3 Jul 2019
- PI Ceramics DurACT Patch Transducer (2022) <https://www.physikinstrumente.com/en/?type=5600&downloadUId=899&downloadFileUId=802> Accessed 5 Jul 2022
- PI Ceramics Material coefficients PIC255 (2023) [https://www.piceramic.com/fileadmin/user\\_upload/physik\\_instrumente/files/datasheets/PI\\_Ceramic\\_Material\\_Data.pdf](https://www.piceramic.com/fileadmin/user_upload/physik_instrumente/files/datasheets/PI_Ceramic_Material_Data.pdf). Accessed Feb 2023
- Saxena S, Sharma R, Pant BD (2017) Dynamic characterization of fabricated guided two beam and four beam cantilever type MEMS based piezoelectric energy harvester having pyramidal shape seismic mass. *Microsyst Technol* 23:5947–5958. <https://doi.org/10.1007/s00542-017-3455-0>
- Sun C, Wang H, Liu J, Shang G (2015) Finite element analysis of vehicle load effect on harvesting energy properties of a piezoelectric unit. *Energy Power Eng* 07:500–508. <https://doi.org/10.4236/epe.2015.710047>
- Umeda M, Nakamura K, Ueha S (1996) Analysis of the transformation of mechanical impact energy to electric energy using piezoelectric vibrator. *Jpn J Appl Phys* 35:3267–3273
- Wang C, Zhao J, Li Q, Li Y (2018) Optimization design and experimental investigation of piezoelectric energy harvesting devices for pavement. *Appl Energy* 229:18–30. <https://doi.org/10.1016/j.apenergy.2018.07.036>
- Wang C, Song Z, Gao Z, Yu G, Wang S (2019) Preparation and performance research of stacked piezoelectric energy-harvesting units for pavements. *Energy Build* 183:581–591. <https://doi.org/10.1016/j.enbuild.2018.11.042>
- Xu X, Cao D, Yang H, He M (2018) Application of piezoelectric transducer in energy harvesting in pavement. *Int J Pavement Res Technol* 11:388–395. <https://doi.org/10.1016/j.ijprt.2017.09.011>
- Yang CH, Song Y, Woo MS, Eom JH, Song GJ, Kim JH, Kim J, Lee TH, Choi JY, Sung TH (2017) Feasibility study of impact-based piezoelectric road energy harvester for wireless sensor networks in smart highways. *Sens Actuators Phys* 261:317–324. <https://doi.org/10.1016/j.sna.2017.04.025>
- Yang Z, Erturk A, Zu J (2017) On the efficiency of piezoelectric energy harvesters. *Extrem Mech Lett* 15:26–37. <https://doi.org/10.1016/j.eml.2017.05.002>
- Yildirim T, Ghayesh MH, Li W, Alici G (2017) A review on performance enhancement techniques for ambient vibration energy harvesters. *Renew Sustain Energy Rev* 71:435–449. <https://doi.org/10.1016/j.rser.2016.12.073>
- Zhao H, Ling J, Yu J (2012) A comparative analysis of piezoelectric transducers for harvesting energy from asphalt pavement. *J Ceram Soc Japan* 120:317–323. <https://doi.org/10.2109/jcersj2.120.317>

**Publisher's Note** Springer Nature remains neutral with regard to jurisdictional claims in published maps and institutional affiliations.